Use of a Variable Energy Penetrometer and Geo-Endoscopic Imaging in the Performance Assessment of Working Platforms...

Conference Paper · June 2016

DOI: 10.1061/9780784479926.110

CITATIONS
0

READS
51

5 authors, including:

Hasan Ahmed Kazmee
University of Illinois, Urbana-Champaign
19 PUBLICATIONS **32** CITATIONS
SEE PROFILE

Erol Tutumluer
University of Illinois, Urbana-Champaign
187 PUBLICATIONS **1,489** CITATIONS
SEE PROFILE

USE OF VARIABLE ENERGY PENETROMETER AND GEO-ENDOSCOPIC IMAGING IN PERFORMANCE ASSESSMENT OF WORKING PLATFORMS CONSTRUCTED WITH LARGE SIZE UNCONVENTIONAL AGGREGATES

Hasan Kazmee[1], and Erol Tutumluer[1], M. ASCE, Younes Haddani[2], Miguel A. Benz Navarrete[2], and Roland Gourves[2]

[1]University of Illinois at Urbana-Champaign, Urbana, Illinois, USA
[2]Sol Solution, Riom Cedex, France

ABSTRACT

Transportation agencies commonly use large size aggregates, often referred to as rock cap or aggregate subgrade, e.g., by Illinois Department of Transportation (IDOT), for stabilizing weak subgrades at wet of optimum moisture states. Adequate characterization of these large rocks is not possible in the laboratory with the use of standard tests. Accordingly, a cone penetration based strength index is the best field assessment tool since shear strength profile is closely linked to unbound aggregate or aggregate subgrade layer performance. To this end, an innovative variable energy dynamic cone penetration (DCP) device, popularly known as PANDA in France, was utilized in a recent Illinois Center for Transportation (ICT) research study involving the performance assessment of large size aggregates over soft subgrades. Twelve full scale working platform sections were constructed with six different types of virgin and recycled large size aggregate materials. Accelerated pavement testing (APT) was carried out on these sections to monitor the rutting progression with number of passes of a certain wheel load assembly. To evaluate layer properties and adequately relate them to rutting performance, PANDA tests were conducted along with traditional DCP soundings on the loading applied pavement test section centerlines. A Geo-endoscopic probe was also used in the holes opened by the PANDA tests to identify layer interfaces and visually document subsurface moisture conditions. The PANDA and Geo-endoscopy testing has proven very beneficial in the performance assessment of the large size aggregate subgrade materials under simulated traffic loading. This paper presents current detailed technical knowledge on the PANDA and Geo-endoscopy test equipment and highlights field results associated with the recent ICT project soundings conducted in the pavement working platform test sections.

Key Words: Large size aggregate, aggregate subgrade, variable energy penetration testing, geo-endoscopy, working platform, accelerated pavement testing.

INTRODUCTION

Maintaining adequate subgrade stability for pavement serviceability and performance has been a major challenge for transportation agencies in the United States. Frost action stemming from harsh winter in Mid-Western and Northern states further exacerbates the situation through frost-heaving and thaw weakening. Thirty percent of total surficial soil in the state of Illinois is hydric in nature indicating permanent or seasonal saturation as experienced in wetlands (USDA 2009). Moreover, Illinois's soils typically have high silt content along with moderate permeability and high suction

potential. As a result, these soils tend to exhibit excessive resilient deformation and frost susceptibility (IDOT Bureau of Bridges and Structures 2005). To mitigate the detrimental effects of freeze-thaw damages, several studies in the early 30's have recommended the use of a free draining thick layer of coarse material up to the extreme depth of frost penetration (Beskow 1947; Taber 1930). Accordingly, inclusion of a thick aggregate layer as frost blanket has been a common practice to ensure stable working platform.

Illinois Department of Transportation (IDOT) has been following a recipe based design approach which determines the thickness of an aggregate cover layer according to subgrade strength. Such a design approach fails to account for the effects of various physical characteristics that govern the granular layer performance itself. Tutumluer et al. (2009) conducted a laboratory study on strength, stiffness and permanent deformation behavior of four different aggregate sources with varying percentages of fines content (percent of dry mass passing through the No. 200 sieve), moisture level and plasticity index. They concluded that such recipe based design approach may not be applicable for marginal quality aggregates like uncrushed gravel or aggregates with plastic fines. In a follow up study by Mishra and Tutumluer (2013), the above finding was corroborated through accelerated pavement testing on full scale construction platforms. Six full-scale test sections were constructed using three different open graded large aggregates varying in size. With reference to the rutting accumulation, these sections outperformed the remaining ones with regular size base course aggregates. However, the findings related to large aggregates from this study was limited in terms of material selection, source, particle size distribution and composition.

IDOT refers to these large rocks as aggregate subgrade that is also used to provide the capillary break for frost susceptible soils. Many other state agencies designates such layers as rock cap materials constituted of crushed virgin aggregates with 76 mm (3 in.) top size. Johnson (1973) conducted a survey on North American agency roadway design practices and reported that Maryland used a 30.5-cm (12 in.) thick granular cap over frost susceptible soils (Johnson 1973). Since 1980, Idaho Department of Transportation has constructed rock cap roadway within an estimated range of 805 to 970 km (500 to 600 miles) (Mathis 1991). In the early 90s, Washington Department of Transportation started to use these large rocks as frost blanket in the highways dedicated to timber freight (Uhlmeyer et al. 2003). In all these applications, the design philosophy predominantly revolved around the use of good quality crushed aggregates from primary sources. More recently, IDOT has introduced three new crushed stone gradation bands namely RR01, CS01 and CS02 to promote enhanced use of large size recycled aggregates as aggregate subgrade materials. The gradation bands allow maximum aggregate sizes as large as 76 to 203 mm (3 to 8 in.). A comparative performance assessment of various rock cap types is needed especially when an asphalt surface course is not provided.

Owing to the dimensional requirements of current standard specifications, conventional laboratory test setups cannot adequately characterize the particle size distributions and strength and modulus characteristics of large aggregate subgrade materials with aforementioned gradations. Similarly, mainstream portable devices like dynamic cone penetrometer, lightweight deflectometer or soil stiffness gauge cannot distinguish the strength and stiffness properties in the field with reasonable accuracy. This paper describes twelve construction platform test sections recently constructed using six different types of aggregate subgrade materials varying in source,

size and composition. Rutting performances of the test sections were monitored periodically from accelerated pavement testing. Successful field applications of a variable energy cone penetration test device and the companion geo-endoscopic imaging are highlighted in this paper for assessing observed rutting performances.

LIMITATIONS OF EXISTING PORTABLE DEVICES

Over the last few decades, various portable devices have been developed to determine in place strength, stiffness and bearing capacity of soils and granular layers. Notably transportation agencies have used Clegg impact hammer, field vane shear test, dynamic cone penetrometer, soil stiffness gauge, seismic pavement analyzer, lightweight deflectometer (LWD) etc. for strength and stiffness characterization. Each of these test methodologies entails certain drawbacks. For example, Clegg impact hammer provides the hardness of surficial soil only; this type of portable device is not feasible for large rocks since the aggregate subgrade may not have a smooth surface due to lack of filler fines. The field vane shear test (VST) is limited to the use in soft clays. The VST is not suitable for cohesionless granular material; since it is impossible to change the load normal to the shear plane. On a similar note, operation of the dynamic cone penetration (DCP) test is physically strenuous and irregular hammer drops can be a potential source of error. Buncher and Christiansen (1992) reported that DCP is prone to skin friction in cohesive soils (Buncher and Christiansen 1992). On a similar note, Webster et al. (1992) recommended to limit the depth of penetration to 30.5 cm (12 in.) in highly plastic soils (Webster et al. 1992). On the other hand, Livneh et al. (1995) documented that angled penetration over a significant depth led to misleadingly higher CBR values (Livneh et al. 1995). Moreover, the penetration indices recorded during the DCP test are dynamic in nature; yet the existing empirical relationships correlate the penetration indices to static CBR values. Majority of the stiffness characterization devices like soil stiffness gauge or LWD have limited depth of influence (Chang et al. 2011). In accordance, such devices are often deemed infeasible for thick granular layers over very soft subgrade. In light of the above discussion, this study evaluated the use of a state of the art penetration device that provides dynamic penetration based strength profiles and visual evaluations with reasonable accuracy over the full depth of proposed construction platforms.

OBJECTIVE AND SCOPE

The primary objective of this paper is to demonstrate the suitability of a variable energy PANDA penetration device and its geo-endoscopic imaging technique for strength assessment of improved subgrade applications. Accordingly, six types of aggregate subgrade materials with varying gradation, source and composition were used to construct twelve construction platform test sections over engineered weak subgrade. An in-place imaging based methodology was developed to determine the particle size and shape properties. During placement and construction of the unsurfaced pavement layers, nuclear density gauge, soil stiffness gauge and lightweight deflectometer were used to assess the density and stiffness of constructed layers. Periodic rut measurements were conducted with increasing number of load applications under accelerated pavement testing (APT). Followed by the completion of APT, PANDA variable energy penetration tests were carried out in and near the center of wheel path in the test sections. Note that the scope of this paper has been limited to the discussion on rutting performances and linkages to strength indices and depths of layer interfaces identified from PANDA soundings. Details of the quality

control test results and imaging based shape characterization can be found elsewhere (Kazmee and Tutumluer 2015).

WORKING PRINCIPLES OF VARIABLE ENERGY PANDA PENETRATION DEVICE

The PANDA^{TM} device by Sol Solution was originally developed at the Blaise Pascal University of Clermont-Ferrand in France based on the principles of an instrumented dynamic cone penetrometer (Gourvès and Barjot 1995). The penetration test is carried out with the impact of a calibrated hammer on an instrumented anvil integrated to an assembly of rods and standardized penetration tip. Figure 1(a) shows the different components of the portable device. Alongside the component designation, parameters critical to the calculation of target strength index are mentioned in parentheses with bold fonts. The calibrated hammer weight is approximately 2 kg (4.4 lbs) and each of the metal rods is 50 cm in length. The stainless steel cone tips are commercially available with two different sizes (2 or 4 cm^2). Since a larger cone tip (4 cm^2) is used to conduct the penetration tests, lateral friction on the rod assembly is assumed to be negligible. As the hammer tended to minimize the rebound impact, the entire amount of applied energy is presumed to reach the cone-tip. Since the primary objective of this study was to present a comparative assessment of selected material strength, this assumption was deemed valid. Strength indices in the form of cone resistance were calculated using the Dutch formula as presented in the following equation according to French standard XP P 94-105.

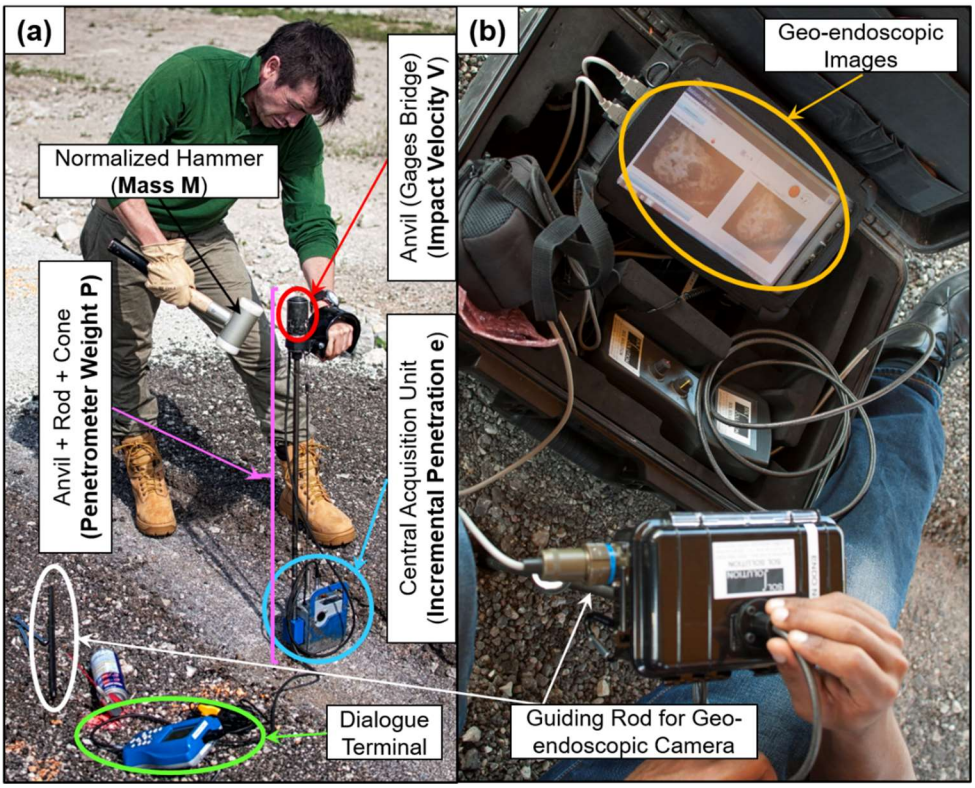

Figure 1: (a) Variable energy PANDA penetration device; (b) Geo-endoscopic Imaging Setup

$$q_d = E \times \frac{1}{Ae} \times \frac{M}{M+P} = \frac{1}{2} MV^2 \times \frac{1}{Ae} \times \frac{M}{M+P}$$

where, q_d = Cone resistance;
A = Cross-sectional area of cone-tip;
M = Mass of the hammer;
V = Impact velocity;
e = Incremental penetration; and
P = Mass of penetrometer assembly (Anvil, rod and cone-tip).

Figure 1(b) shows the geo-endoscopic imaging setup that is used for identification of layer interfaces and depth of water table. After finishing the penetration test, a perforated guiding rod is shoved into the ground through that same borehole. An endoscopic camera having 6 mm diameter is lowered into the cavity of that guiding rod. The endoscope continuously record the surrounding images of borehole wall in 640 X 480 pixels at 10 X magnification. The length of electronic guiding cable attached to the endoscope may act as a reference to the depth of the borehole. This imaging technique has already been successfully implemented in railway geotechnics as well as in substructure integrity assessment (Llanca et al. 2013; Mishra et al. 2015). Apart from identification of layer interfaces, the geo-endoscopy has also been utilized for establishing particle size distribution of sandy gravel (Breul and Gourves 2006).

DESIGN AND CONSTRUCTION OF FULL SCALE TEST SECTIONS

This section presents a brief description on the particle size distributions of selected aggregate subgrade materials in conjunction with the design layout of proposed test sections. The designed test sections were constructed over weak subgrade engineered to a controlled strength of either CBR = 1% or 3%. Details of the subgrade strength engineering can be found elsewhere (Kazmee et al. 2015).

Aggregate Materials Used

The aggregate subgrade and capping aggregate materials used in this study were all representative of those commonly used by IDOT districts. Figure 2 shows the particle size distributions of aggregate subgrade and capping materials that were used during the construction. Types A through D and Type F aggregates constituted of large rocks much greater in size than typical base course top size (25 mm [1 in.]) aggregates; whereas, Type E and Type G were regular base course type aggregates fitting the IDOT coarse aggregate CA06 gradation band. The major difference between these two aggregate types was the dissimilarity in source composition; Type G originating from virgin primary sources and Type E sourced from reclaimed asphalt pavement (RAP) materials. Due to the presence of inherent moisture and asphalt binder, finer particles in RAP exhibited clumping tendency and thus had lower fines content than Type G dolomite. Among the aggregates with large rocks, Type F crushed stones (IDOT CA02) were commonly more well-graded with approximately 4% of fines. Contrary to that Type C primary crusher run aggregates were the coarsest and very uniformly graded with a top size of 203 mm (8 in.). Type A was a rip-rap size aggregate with 62.5 mm (21/2 in.) top size loosely fitting the IDOT gradation requirement of RR01. This particular virgin aggregate had a negligible amount of filler material (fines/materials passing through the No. 200 sieve), with only 10% material passing through a 19 mm (3/4 in.) sieve. Both Type B and Type D aggregates were from reclaimed sources with varying percentages of recycled concrete aggregates (RCA). Even though these two aggregate types were proposed to replicate the IDOT CS01 gradation band; the coarser portion of the particle size distributions of these two aggregates did not fit in the target gradation envelope. Type D aggregates had a 60%-

40% blend of RCA and RAP with a gradation significantly finer than Type B (100% concrete demolition waste).

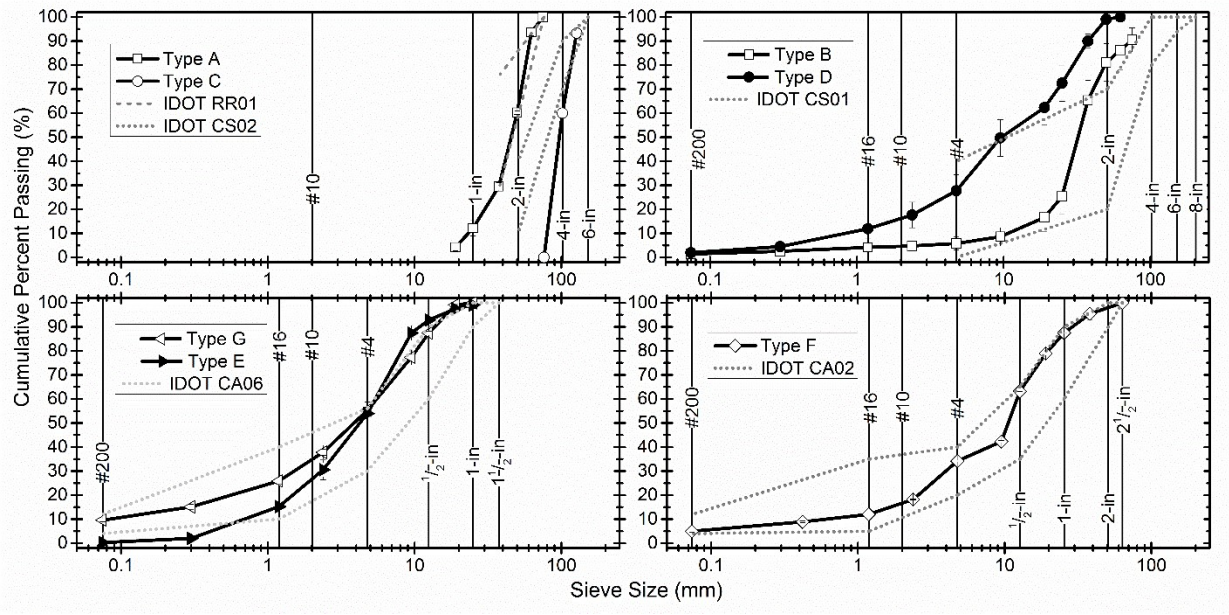

Figure 2: Particle size distributions of selected aggregate subgrade and subbase materials

Layout of Test Sections

According to the proposed design, the entire test road was divided into three equal length cell blocks namely Cells 1, 2 and 3. Cells 1 and 2 working platform sections were constructed over CBR = 1% to validate the adequacy of large rocks for improved subgrade applications. On the other hand, Cell 3 test sections constructed with conventional size unbound granular materials had an engineered subgrade strength of CBR = 3%. Each of these cells had four working platform sections constructed with two different aggregate subgrade and two different capping materials. The full scale test sections were designed in a way so that an Advanced Transportation Loading ASsembly (ATLAS) APT equipment could load all four test sections in each cell at the same time.

Figure 3 presents a three-dimensional view of the designed Cells. In Figure 3, numbers in parentheses next to material type indicate the corresponding cell number. Each test section was assigned three distinct Roman numerals (separated by slashes). The first numeral indicates the test section if that was constructed in Cell 1; the second numeral stands for the section number constructed in Cell 2. Similar nomenclature is applicable for the test section constructed in Cell 3. All the odd numbered sections had Type G dolomite capping; meanwhile, all the even numbered sections had Type E RAP capping.

Each of the test sections was 4.6 m long and 2.7 m wide. Two consecutive sections with the same aggregate subgrade had dolomite (Type G) and RAP (Type E) capping, respectively. Design thicknesses were assigned in accordance with IDOT Subgrade Stability Manual (Bureau of Bridges and Structures 2005). Since the large size rocks had significant voids in the granular matrix, a 7.6 cm (3 in.) thick regular base course capping layer was provided to confine the large rocks with a finished surface. Right in the middle of each cell, a 3.1 m long transition zone was

provided so that the interface effect could be avoided during the accelerated pavement testing. A unidirectional loading of 44.5 kN (10 kip) (equivalent contact pressure 758 kPa [110 psi]) applied repeatedly with a super-single tire being pulled at a constant speed of 8 km/h (5 mph). Note that a 9.1 m long buffer zone was provided at both ends of each cell so that the ATLAS crawler could be placed properly and a constant speed could be maintained during the APT. The dotted line on the platform surface in Figure 3 denotes the span over which rutting measurements were taken at an interval of 5 cm (2 in.). The dashed lines designate the two measurement locations equally spaced from each other and the section boundary. The circle highlighted as the QC test spot on the surface indicates the center point of each section near which all the quality control tests and PANDA soundings were carried out.

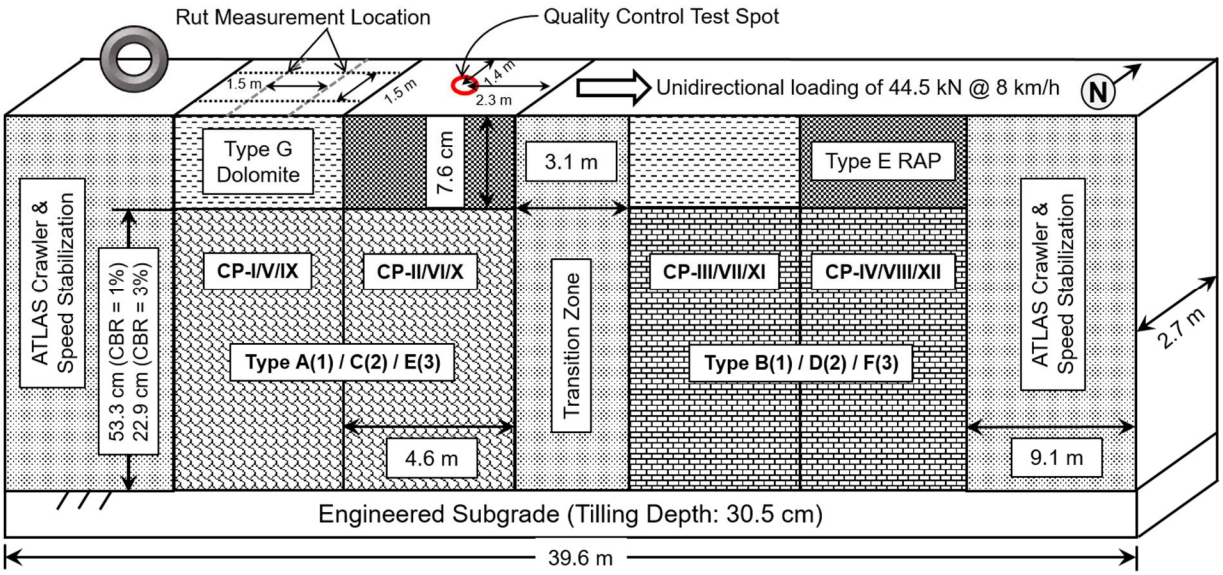

Figure 3: Three dimensional view of constructed test sections

SUBSTRUCTURE PROFILES FROM DCP, PANDA AND GEO-ENDOSCOPY TESTING

Numerous previous studies have linked shear strength of granular materials to corresponding rutting performance (Saeed 2008). Henceforth, in place strength assessment of these large rocks was deemed critical for the investigation of rutting performances. Alongside PANDA, dynamic cone penetration (DCP) tests were also conducted to cross-check the penetration pattern recorded by the variable energy penetration device. A well-established correlation by Kleyn et al. (1982) was used to calculate the California Bearing Ratio (CBR) values from DCP penetration indices (Kleyn et al. 1982). Figure 4 shows the recorded cone resistances and CBR values in different sections of Cell 1. The gray colored solid horizontal lines identify the layer interfaces revealed from trenching of those sections. The depths of water table encountered by geo-endoscopy are also indicated. Figure 4 also shows several of the geo-endoscopic images recorded at different depths of those sections. The solid line strength profiles show the cone resistances in different sections; whereas, the dark grey dashed lines present the CBR values from DCP tests.

Comparing the responses from PANDA and DCP, one significant difference can be noted. Right at the interface between aggregate subgrade and the engineered subgrade, DCP exhibited abrupt shifts in CBR values; whereas, such change was more gradual in case of PANDA cone resistances. Closer inspection to the trenched sections (after completion of accelerated pavement testing) revealed that the large rocks of aggregate subgrade and the weak engineered subgrade tended to migrate at different phases of the construction. As a result, an intermixed layer emerged in each of the large rock sections. Considering certain erosion potential or drainage issues in absence of geosynthetic separation layer, a quantifiable extent of intermixing is extremely important for the long term maintenance plan. To this end, the variable energy PANDA penetrometer can be more beneficial than the traditional DCP. For example, the DCP exhibited a penetration index of 10 cm/blow at 70 cm. Conversely, from 55 to 65 cm depth, the PANDA penetrometer exhibited gradual decrease in cone resistance followed by an increase up to a depth of 70 cm. This indicated the presence of large rocks migrated into the soft engineered subgrade. Despite the concern for layer contamination, such intermixing was proven to be beneficial for improved subgrade applications overall.

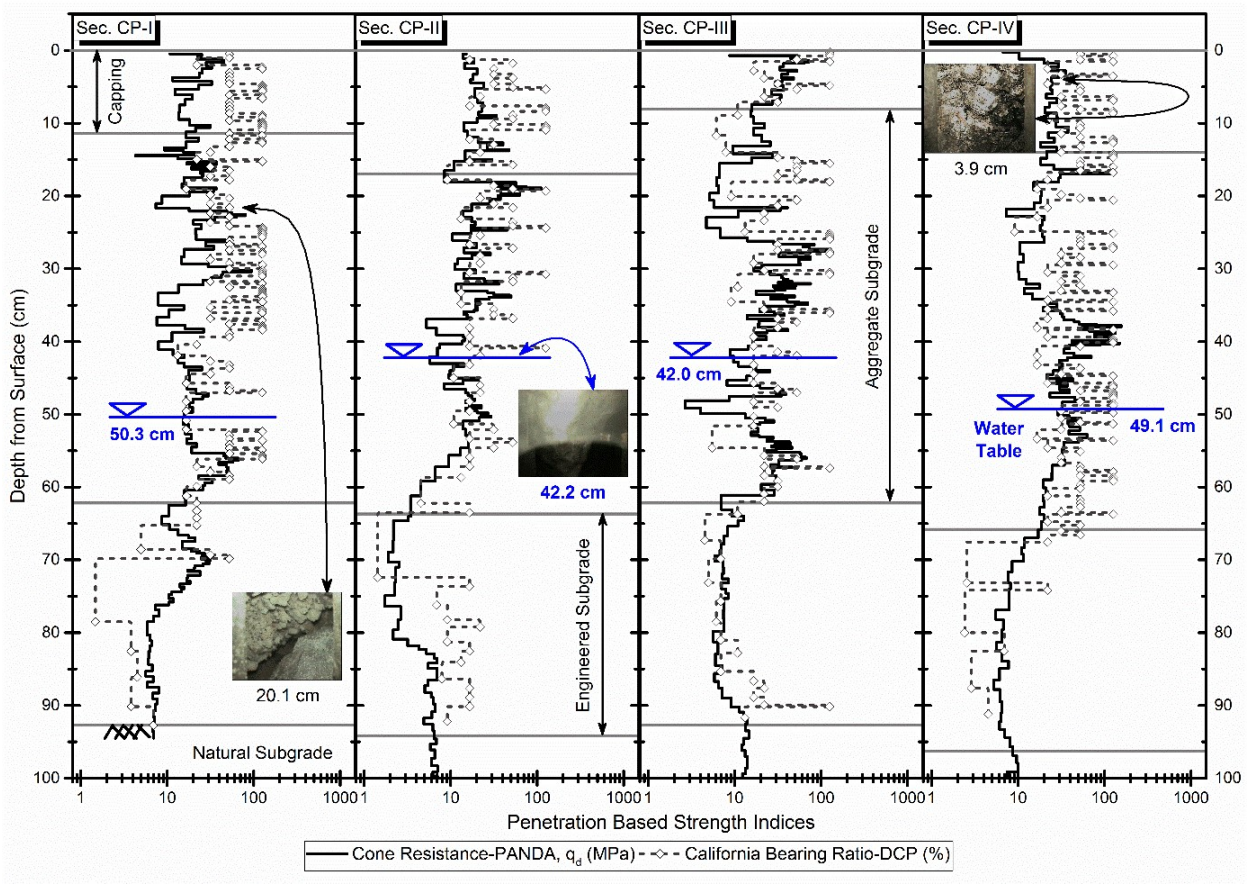

Figure 4: Penetration based strength indices recorded in Cell 1 test sections (Section CP-I through Section CP-IV)

The improvement in subgrade strength was also notable from both PANDA and DCP tests. Although the sections in Cell 1 were constructed over CBR = 1% subgrade, three out of the four

sections exhibited 8 to 10 times higher than the design subgrade strength. The geo-endoscopic imaging suggested that there might have been a water pocket in Sections CP-II and CP-III. Both of these sections exhibited very similar and shallower depth of water table; whereas, water tables in the remaining two sections were found to be deeper. Presence of shallower water table affected the strength indices of Section CP-II more than those of Section CP-III. Note that Type B aggregate subgrade in Section CP-III was comparatively finer than Type A aggregate subgrade. As a result, the higher grain to grain contact superseded the detrimental effect of pore pressure leading to a stronger granular layer below the water table. The effect of voids in granular matrix was also evident from the comparative assessment of strength indices in the capping layer and the aggregate subgrade layer. For instance, the cone resistance in capping layer of Section CP-III was found to be in the range of 27 MPa to 72 MPa. On the contrary, cone resistance in the aggregate subgrade layer varied in between 3 MPa to 109 MPa. The even numbered sections had higher capping thicknesses compared to the odd numbered sections in Cell 1. Because of the space constraint, strength profiles over the entire working platform depth in Cell 2 and Cell 3 sections are not presented in this paper. Relevant information can be found in a previously published research report (Kazmee and Tutumluer 2015).

VALIDATION OF RUTTING PERFORMANCE WITH PANDA PENETRATION DEVICE AND GEO-ENDOSCOPY

To evaluate the efficiency of strength characterization with variable energy PANDA penetrometer, all the relevant layer thicknesses, depths of water table, cone resistance values in different layers of the construction platforms were plotted in a single graph as shown in Figure 5. Figure 5(a) presents the measured rut accumulations after 4,000 wheel passes (or obtained at failure at a wheel path rut depth of approximately 76 mm or 3 in). Unless indicated otherwise (over the y-axis on right side of the figure), all remaining construction platform sections survived 4000 passes. On the basis of the accumulated rutting results, Type D aggregate subgrade sections showed the best performance.

Individual layer thicknesses in different test sections are presented in Figure 5(b). Total aggregate cover thicknesses were found to be the highest in Section CP-VII and Section CP-VIII. Both of these sections had the same Type D aggregate subgrade with alternating capping layers of Type G and Type E, respectively. Owing to the thicker aggregate cover, Type D aggregate subgrade sections accumulated the least amount of rutting among all the sections. The influence of thickness can be further illustrated by the performance comparison of Cell 3 test sections. As the total aggregate cover decreased from Section CP-IX to Section CP-XII, number of passes to reach the designated failure limit also decreased. Despite the fact that Cell 3 sections were constructed over a comparatively stronger subgrade; the additional aggregate cover thickness in Cell 1 and Cell 2 working platform sections resulted in better rutting performance.

Consistent with results presented in Figure 4, the even-numbered sections had thicker capping layers than the odd-numbered sections in the other two cell blocks. In spite of the thicker capping layers, the RAP capped sections either exhibited higher magnitude of rutting or survived fewer passes to reach failure. This finding substantiates RAP's susceptibility to rutting as claimed by several other research studies (Dong and Huang 2014; Garg and Thompson 1996). Even with slightly thicker aggregate cover and similar water table, Section CP-II underwent shear failure in comparison to Section CP-III enduring 4,000 passes.

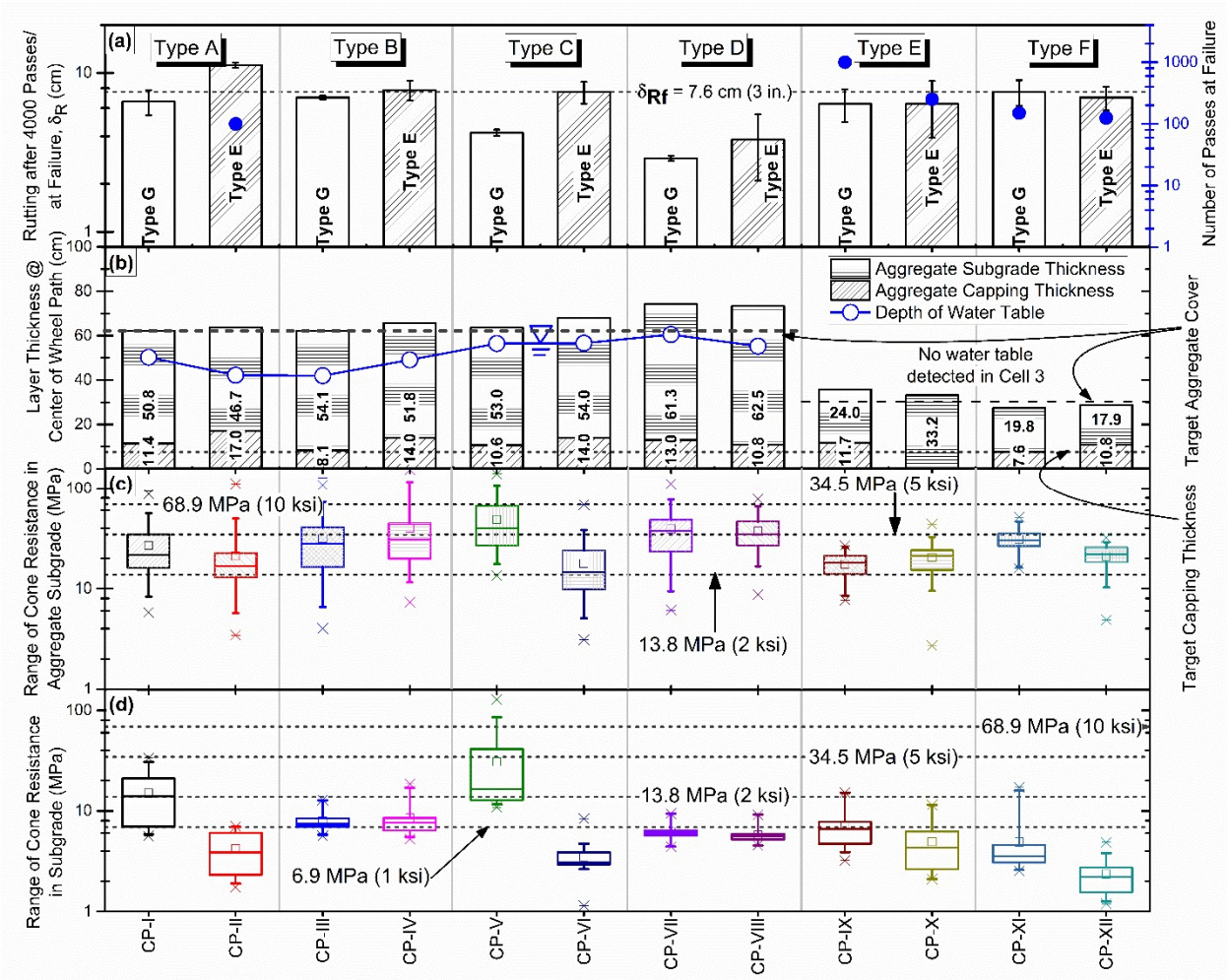

Figure 5: As-constructed granular layer thicknesses, strength indices, depths of water table and rutting performances of working platform test sections.

The effect of moisture on rutting performance was also investigated using the depths of water table identified from geo-endoscopic imaging. As presented in Figure 5(b), the shallowest water table was detected at Section CP-II and Section CP-III, and the deepest water table was detected at Section CP-VII. As mentioned in the previous section, the effect of the shallow water table was more severe in the uniformly graded aggregates than in the somewhat well-graded aggregates. That's why, Section CP-II, which had uniformly graded Type A riprap size aggregate subgrade, failed prematurely at 100 passes. A deeper water table was found to be favorable for low rutting accumulation. For example, Section CP-VII, which had the deepest water table, accumulated the least permanent deformation after 4,000 passes among all the test sections.

Regardless of the considerable variation in aggregate cover thickness and water table, the best way to compare corresponding aggregate subgrade material performance is to inspect the distribution of strength over the depth of construction platform. To this end, box-whisker plots for the range of cone resistance in the aggregate subgrade and engineered subgrade layers are presented in Figure 5(c) and 5(d), respectively. Type E RAP exhibited the lowest cone resistance

among all the aggregate subgrades. This observation conforms to the poor rutting performance of RAP capped sections. Type D aggregate subgrade exhibited significantly higher cone resistance in comparison to the other types because of denser packing. Section CP-V constructed with Type G capping stone and Type C aggregate subgrade registered the highest cone resistance among all the sections. On the contrary, cone resistance also varied over a wide span due to voids in granular matrix. The significance of denser packing becomes evident by judging rutting performances in section CP-VI. Despite the sheer size of primary crusher run Type C aggregates, large voids in granular matrix contributed to very low cone resistance in aggregate subgrade layer of section CP-VI. Disparity in strength indices was also another problem for such uniformly graded materials. Another important observation is that in the RAP capped sections with large rocks and limited filler materials (e.g. Type A, C and F), the engineered subgrade did not exhibit cone resistance as high as that of the dolomite counterparts. This infers that the viscous nature of RAP might have been contributing to the absorption of some of the compaction energy during construction; thereby, the intended benefits of intermixing through large rock migration were absent in those sections.

CONCLUSIONS

A field study was undertaken at the Illinois Center for Transportation established at the University of Illinois to validate newly introduced Illinois DOT gradation bands for large siz unconventional aggregate subgrade materials for improved subgrade applications. Twelve full scale test sections were constructed and tested for rutting accumulation using an accelerated pavement testing device. A state-of-the-art variable energy penetration device PANDA was used for a comparative strength characterization of selected materials. Geo-endoscopic imaging technique was also implemented to examine the layer interfaces and depths of water table. Findings from these PANDA testing and geo-endoscopy imaging helped to properly investigate the field rutting trends observed in the constructed test sections. Significant improvement in subgrade strength was noticed in the test sections with large rocks constructed over a very weak subgrade with a controlled strength of CBR = 1%. Application of reclaimed asphalt pavement (RAP) aggregates for improved subgrade should be dealt with caution since the RAP capped sections were found to be susceptible to rutting.

REFERENCES

1. Beskow, G. (1947). "Soil freezing and frost heaving with special application to roads and railroads." *Soil Science,* 65(4).
2. Breul, P., and Gourves, R. (2006). "In field soil characterization: approach based on texture image analysis." *Journal of Geotechnical and Geoenvironmental Engineering,* 132(1), 102-107.
3. Buncher, M. S., and Christiansen, D. J. (1992). "USAF's new contigency soils/pavement testing van." *Proceedings of the Conference on Road and Airport Pavement Response Monitoring Systems,* West Lebanon, NH, 27-40.
4. Bureau of Bridges and Structures. (2005). *Subgrade Stability Manual.* Illinois Department of Transportation, Springfield, IL.
5. Chang, G., Xu, Q., Rutledge, J., Horan, B., Michael, L., White, D., and Vennapusa, P. (2011). "Accelerated implementation of intelligent compaction technology for embankment subgrade soils, aggregate base, and asphalt pavement materials." *Rep. No. FHWA-IF-12-002,* Federal Highway Administration, Washington, DC.
6. Dong, Q., and Huang, B. (2014). "Laboratory evaluation on resilient modulus and rate dependencies of RAP used as unbound base material." *Journal of Materials in Civil Engineering,* 26(2), 379-383.

7. Garg, N., and Thompson, M. R. (1996). "Lincoln Avenue reclaimed asphalt pavement base project." *Transportation Research Record: Journal of the Transportation Research Board,* 1547(1), 89-95.
8. Gourvès, R., and Barjot, R. (1995). "The PANDA ultralight dynamic penetrometer." *Proceedings of the XI European Conference on Soil Mechanics and Foundation Engineering,* Copenhagen, Denmark, 83-88.
9. Johnson, T. (1973). "North American practice in design of roads in seasonal frost areas." *Proceedings of the Symposium on Frost Action on Roads,* Norwegian Road Research Laboratory, Oslo.
10. Kazmee, H., Mishra, D., and Tutumluer, E. (2015). "Sustainable alternatives in low volume road base course applications evaluated through accelerated pavement testing." *Proceedings of The 2015 International Foundations Congress and Equipment Exposition,* American Society of Civil Engineers, San Antonio, TX, 409-418.
11. Kazmee, H., and Tutumluer, E. (2015). "Evaluation of aggregate subgrade materials used as pavement subgrade/granular subbase." *Rep. No. FHWA-ICT-15-013,* Illinois Department of Transportation, Springfield, IL.
12. Kleyn, E., Maree, J., and Savage, P. F. (1982). "The application of portable pavement dynamic cone penetrometer to determine in situ bearing properties of road pavement layers and subgrades in South Africa." *Transportation Research Record: Journal of the Transportation Research Board,* (Accession Number: 00390298).
13. Livneh, M., Ishai, I., and Livneh, N. A. (1995). "Effect of vertical confinement on dynamic cone penetrometer strength values in pavement and subgrade evaluations." *Transportation Research Record: Journal of the Transportation Research Board,* (1473), 1-8.
14. Llanca, D., Breul, P., Bacconnet, C., and Sahli, M. (2013). "Characterization of the masonry lining of an underground structure by geoendoscopy." *Tunnelling and Underground Space Technology,* 38 254-265.
15. Mathis, D. (1991). "Rock Cap: A True Free Draining Base." *Proceedings of 42nd Annual Road Builders' Clinic,* Coeur D'Alene, ID, 153-156.
16. Mishra, D., Gallier, J., Tutumluer, E., Haddani, Y., and Gourves, R. (2015). "Application of PANDA and geo-endoscopy techniques for improved assessment of track substructure conditions at railroad bridge approaches." *Proceedings of the 2015 Joint Rail Conference,* American Society of Mechanical Engineers, San Jose, CA, 1-8.
17. Mishra, D., and Tutumluer, E. (2013). "Field Performance Evaluations of Illinois Aggregates for Subgrade Replacement and Subbase - Phase II." *Rep. No. FHWA-ICT-12-021,* Illinois Department of Transportation, Springfield, IL.
18. Saeed, A. (2008). *Performance-related tests of recycled aggregates for use in unbound pavement layers.*
19. Taber, S. (1930). "The mechanics of frost heaving." *The Journal of Geology,* 38(4), 303-317.
20. Tutumluer, E., Mishra, D., and Butt, A. (2009). "Characterization of Illinois Aggregates for Subgrade Replacement and Subbase." *Rep. No. FHWA-ICT-09-060,* Illinois Department of Transportation, Springfield, IL.
21. Uhlmeyer, J., Pierce, L., Lovejoy, J., Gribner, M., Mahoney, J., and Olson, G. (2003). "Design and construction of rock cap roadways: Case study in Northeast Washington State." *Transportation Research Record: Journal of the Transportation Research Board,* (1821), 39-46.
22. USDA. (2009). "Hydric Soil Distribution in Illinois." http://www.nrcs.usda.gov/Internet/FSE_MEDIA/stelprdb1167160.jpg .
23. Webster, S. L., Grau, R. H., and Williams, T. P. (1992). "Description and application of dual mass dynamic cone penetrometer." *Rep. No. Report GL-92-3,* Department of the Army, Washington, DC.